Supporting Information

Redox-driven confinement of quinone with imidazole in sub-nanometer sized porous carbon space mitigating chemical degradation for aqueous energy storage

Jeehae Yang,‡[a] Anseong Park,‡[b] Taesung Kwon,[c] Yongkyu Lee,[b] Won Bo Lee,[b]* Ki Min Nam,*[c] YongJoo Kim*[d] and Jinho Chang*[a]

[a]Department of Chemistry and Research Institute for Convergence of Basic Science, Hanyang University, Seoul 04763, Republic of Korea

[b]School of Chemical and Biological Engineering and Institute of Chemical Processes, Seoul National University, Seoul 08826, Republic of Korea

[c]Department of Chemistry and Chemistry Institute of Functional Materials, Pusan National University, Busan 46241, Republic of Korea

[d]Department of Materials Science and Engineering, Kookmin University, Seoul 02707, Republic of Korea

*** E-mail address**

Jinho Chang: jhcechem@hanyang.ac.kr

YongJoo Kim: cjyjee@kookmin.ac.kr

Ki Min Nam: namkimin.chem@gmail.com

Contents

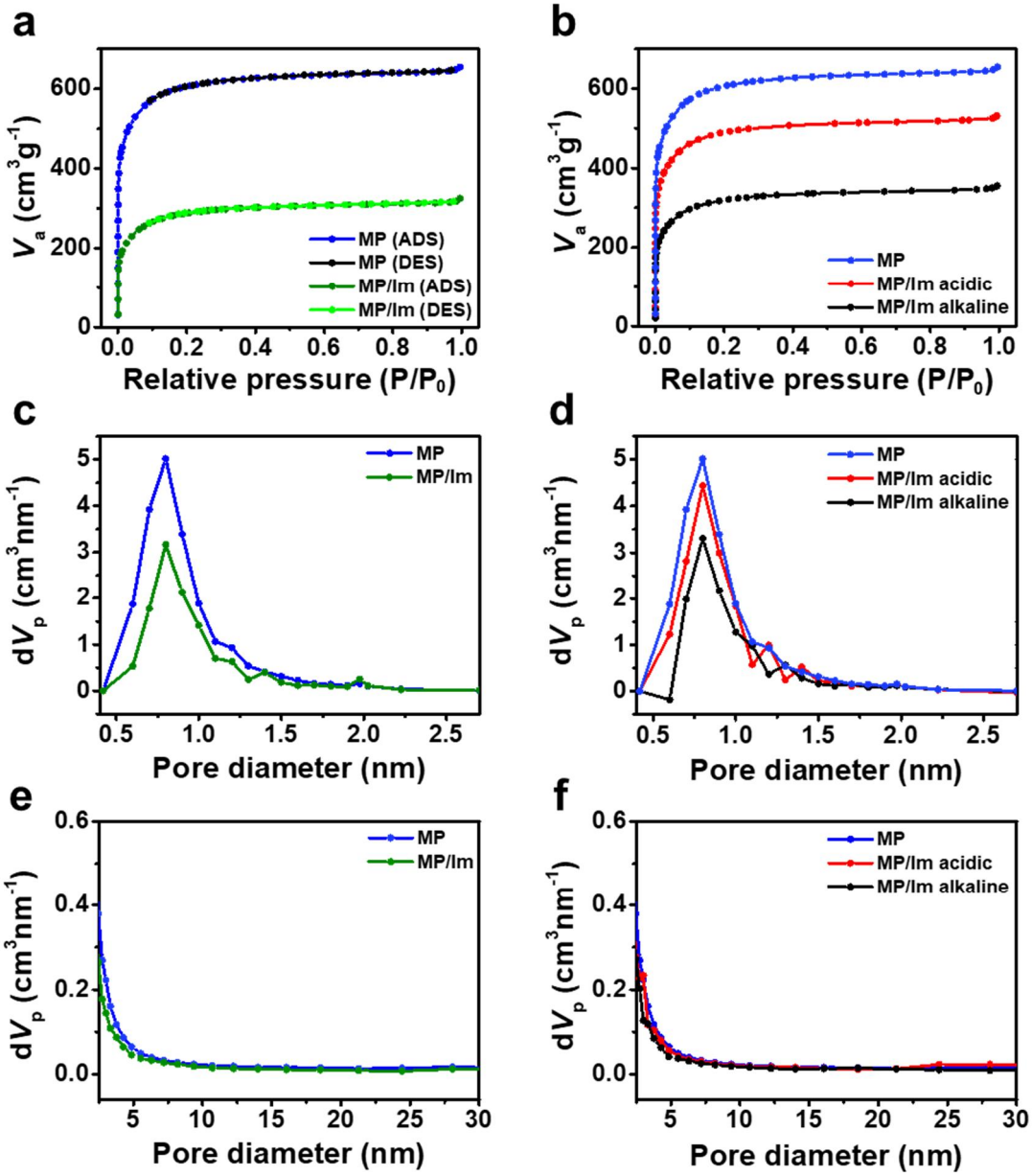

Figure S1. (a) N_2 absorption/desorption isotherms for the pristine microporous carbon (MP) and the one immersed in 1M im solution (MP/Im) at pH ~ 7. (b) N_2 absorption isotherms for MP, MP/Im acidic (the solution pH ~ 1), and MP/Im alkaline (the solution pH ~ 13). Micropore size distributions of (c) MP and MP/Im, (d) MP, MP/Im acidic, and MP/Im alkaline. Mesopore size distributions of (e) MP and MP/Im, (f) MP, MP/Im acidic and MP/Im alkaline.

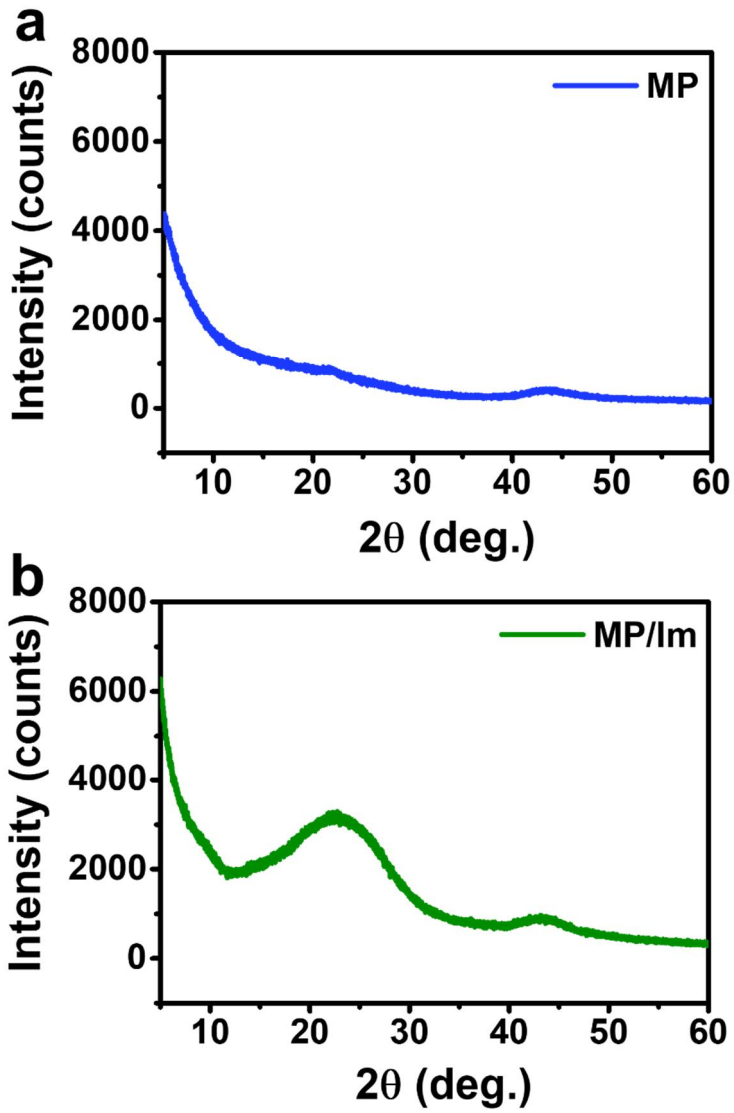

Figure S2. XRD of (a) the microporous carbon and (b) the microporous carbon immersed in the 1 M Im solution at pH ~ 7.

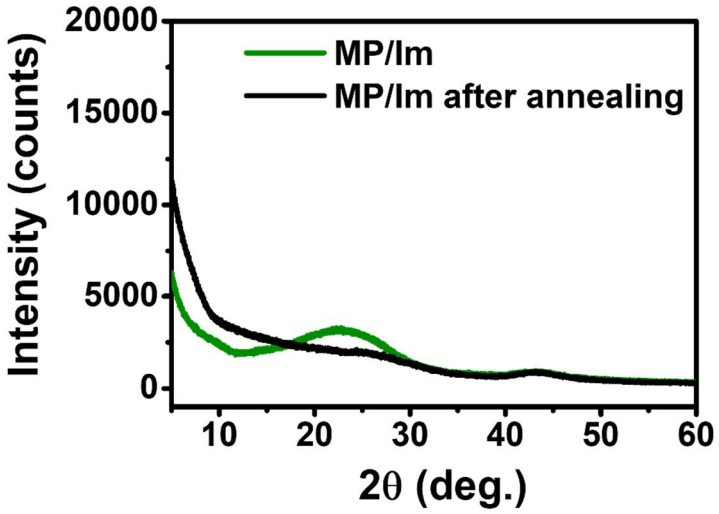

Figure S3. XRD of the microporous carbon immersed in the 1 M Im solution at pH ~ 7 (green) and after annealing at 300 ^{o}C (black).

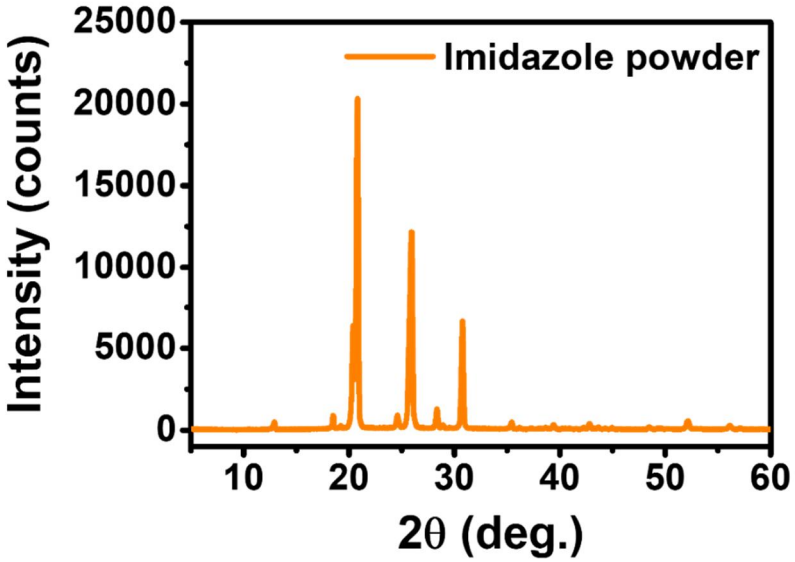

Figure S4. The XRD of Imidazole powder.

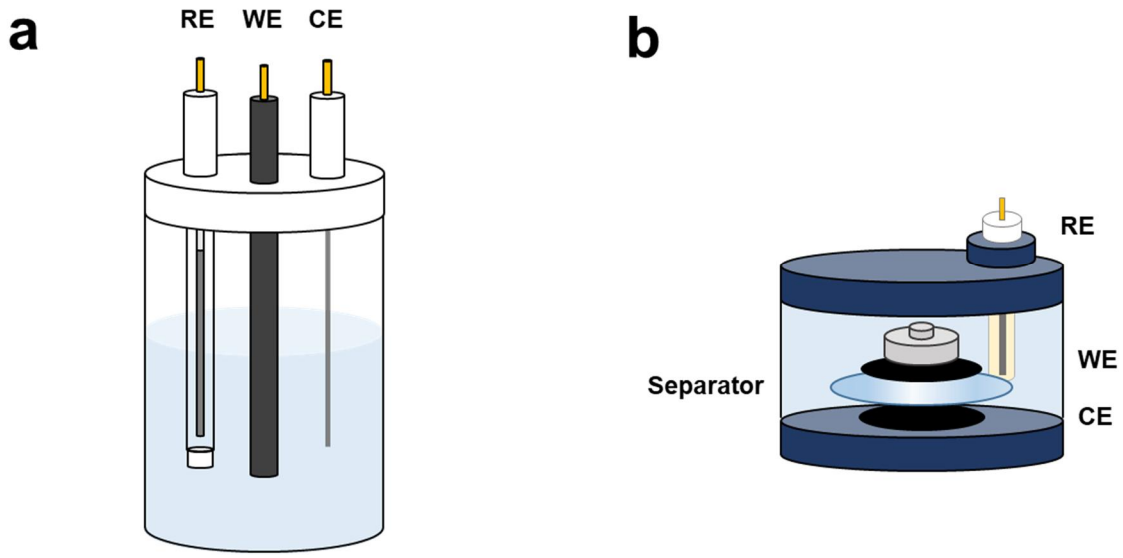

Figure S5. Schematic descriptions of (a) an open- and (b) a compact-cell.

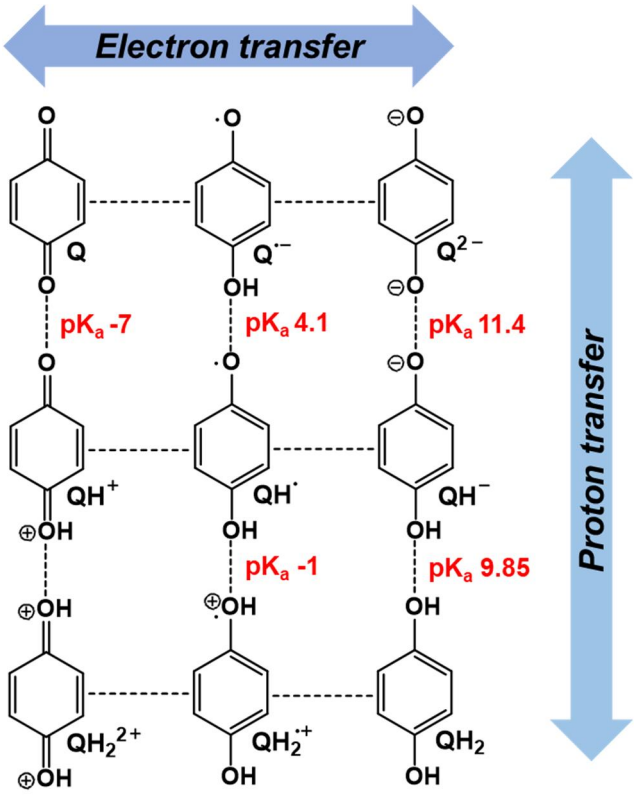

Figure S6. The nine squared scheme of H_2Q/Q redox reaction via proton-coupled electron transfers (PCETs), and the corresponding pK_a values reported.[1]

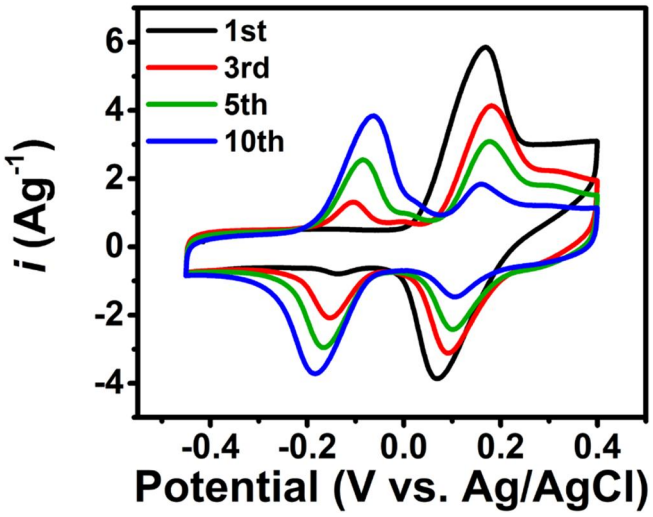

Figure S7. Successive CVs (1, 3, 5, and 10th cycle) at 5 mV/s measured in the compact-cell configured as MPE (CE)|5 mM H_2Q + 1 M Im, pH ~ 7||the same electrolyte condition as the other side|MPE (WE).

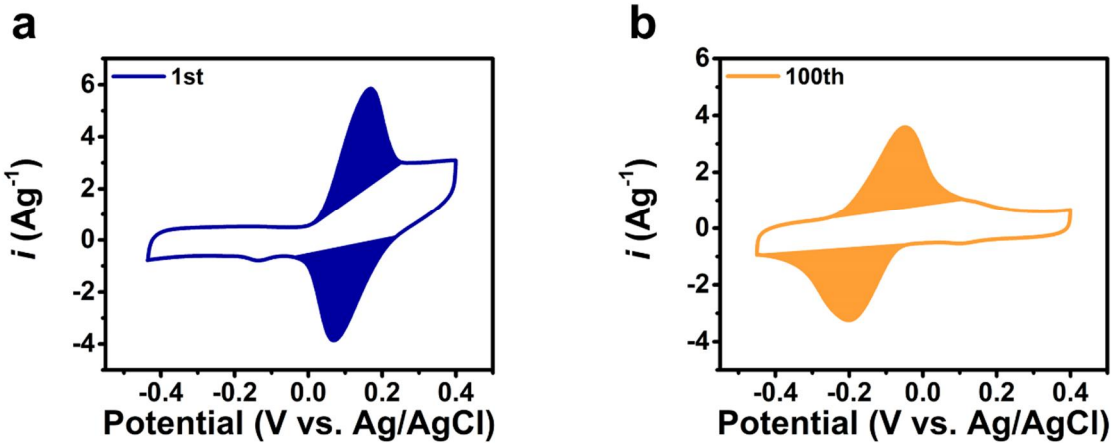

Figure S8. Integrated voltammetric areas to estimate charges for H_2Q oxidation to Q and vice versa at (a) 1st and (b) 100th cycle. Both anodic and cathodic peak areas from 1st and 100th cycle CVs were estimated to be 90.5 and 87.0 C/g, respectively; the volume of the electrolyte in the compact cell was 240 μL, and the theoretical charge for the complete electrolysis of H_2Q and vice versa was 95.8 C/g.

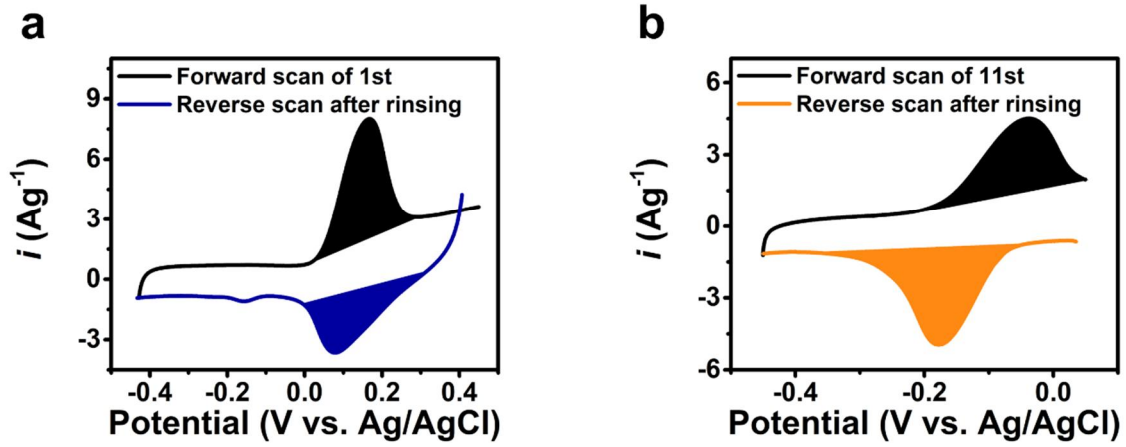

Figure S9. (black) Forward scanned voltammogram for electrolytic oxidation of H_2Q from the (a) 1st and (b) 11th CV cycle. After that, each the compact-cell was dissembled, and MPE was rinsed with deionized water and immersed in the 1 M Im solution without H_2Q for 1 hour. Negatively swept voltammogram for reduction of (a, blue) residual Q and (b, orange) $Quinone_{Ox,Confined}$ in the MPE.

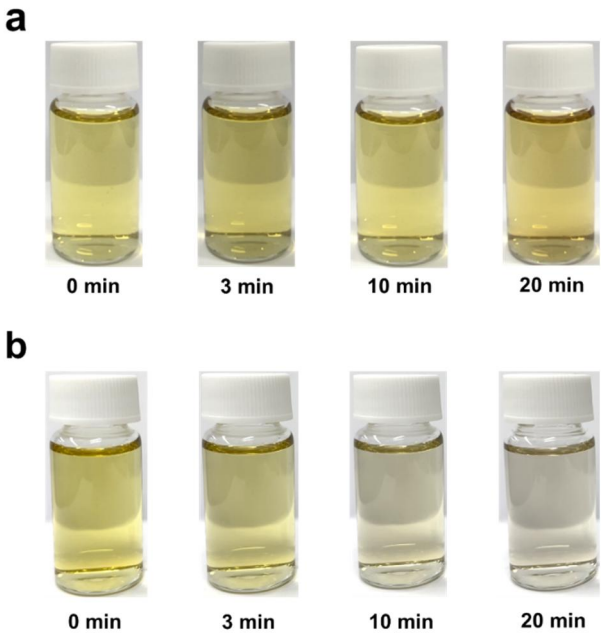

Figure S10. Snapshots for the transiently observed color change of the 5 mM Q solutions (a) without and (b) with 1 M Im for 20 minutes.

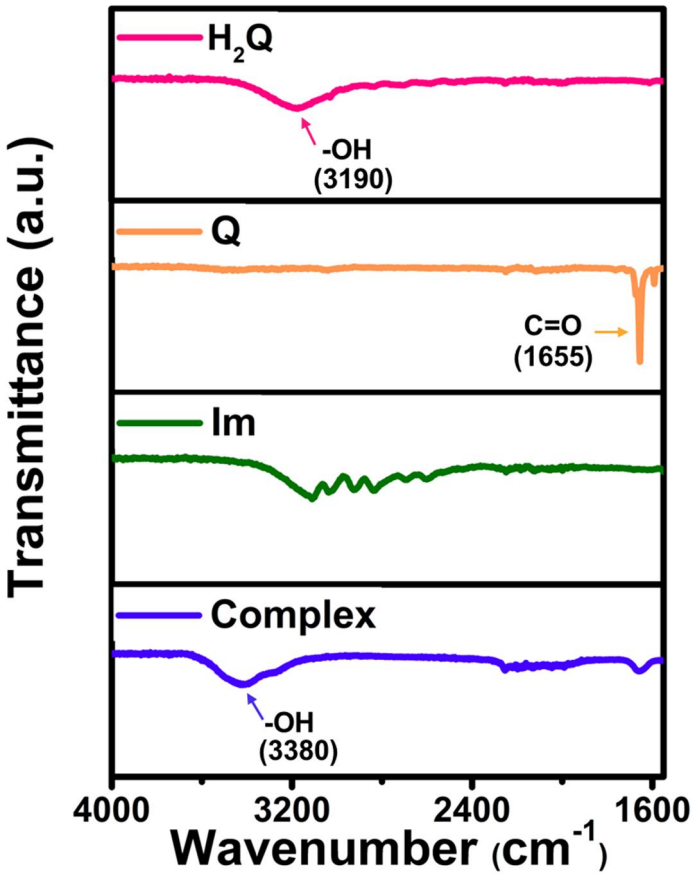

Figure S11. ATR-FTIR spectra of H_2Q, Q, Im and the quinone-Im complex dissolved in DMSO-d_6.

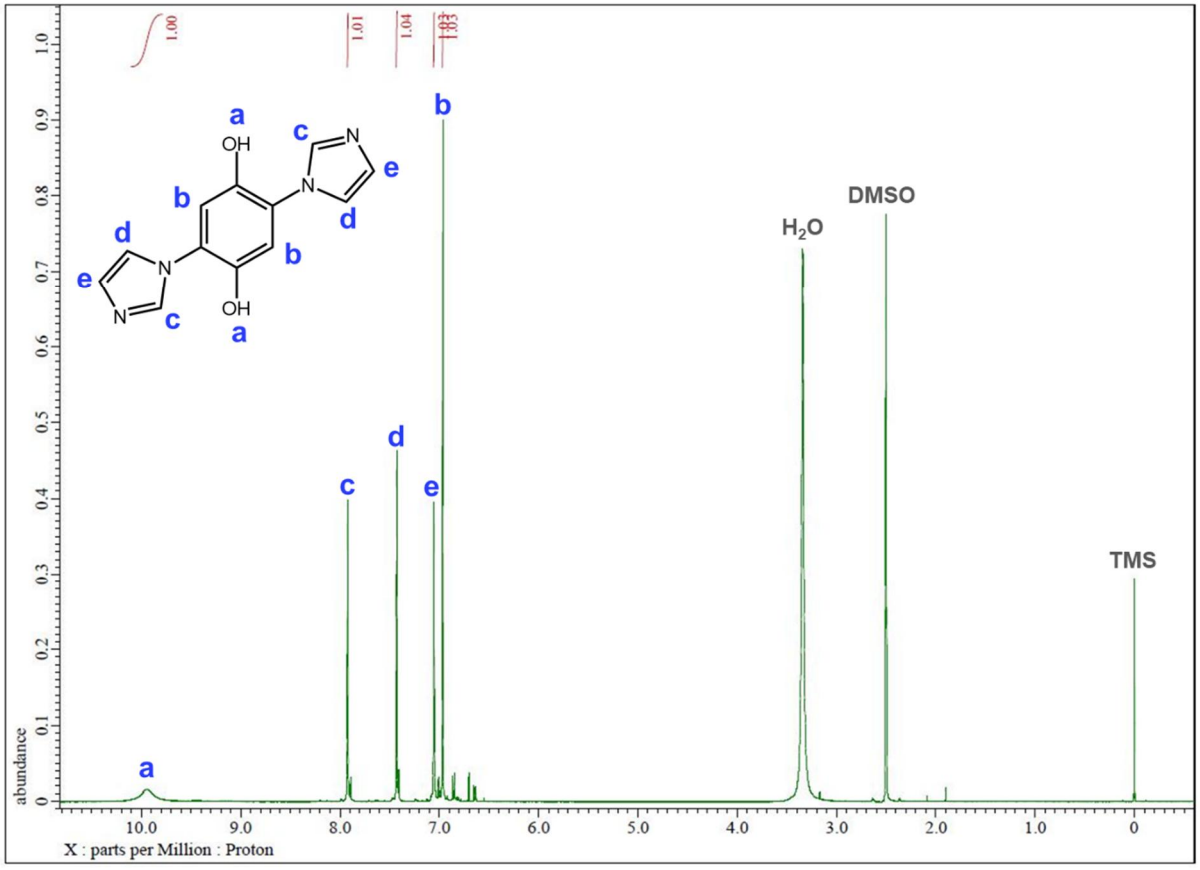

Figure S12. ^{1}H NMR spectrum of the quinone-Im complex: ^{1}H NMR (500 Hz, DMSO-d_6) δ (ppm) = 9.93 (s, 2H), 7.92 (s, 2H), 7.43 (s, 2H), 7.05 (s, 2H), and 6.97 (s, 2H).

Note S1. Voltammetric estimation for the reaction order of Q in its homogenous reaction with Im.

Figure S13a–c shows the successive CVs on a Pt ultramicroelectrode (UME) with its radius, a = 5 μm measured in aqueous solutions with Q at different concentrations (2.5, 5 and 10 mM) after the injection of Im to 1 M. It was clearly shown that the cathodic limiting current ($i_{lim,c}$) by electro-reduction of Q decreased, while the anodic one by electro-oxidation of H_2Q increased. $i_{lim,c}$ under the diffusion on an UME is defined as follows:[2]

$$i_{lim,c} = 4nFC_Q^*D_Qa \quad \text{(S1)}$$

Here, n = 2 is the e^- number for the electro-reduction of Q, F is the Faraday constant, and C_Q^* and D_Q are the bulk concentration and the diffusion coefficient of Q, respectively. From the measured $i_{lim,c}$ over time, the C_Q^*-t profiles with different initial concentration values were measured, as shown in Figure 1h. Because the concentration of Im was more than two orders of magnitude higher than that of Q, the chemical reaction between Q and Im was considered a pseudo-first-order reaction, the rate of which is expressed as follows:

$$Rate = k'[Q] \quad \text{(S2)}$$

The initial rates of the chemical reaction at different concentrations of Q were estimated from the slopes of the C_Q^*-t profiles from 0 to 40 s, which are listed in Table S2. The reaction order of Q was estimated to be 1 based on the measured initial reaction rates, and the corresponding average pseudo-first order rate constant (k') was estimated to be 5.18×10^{-3} s^{-1}. The calculated lifetime of Q ($1/k'$) was 193 s.

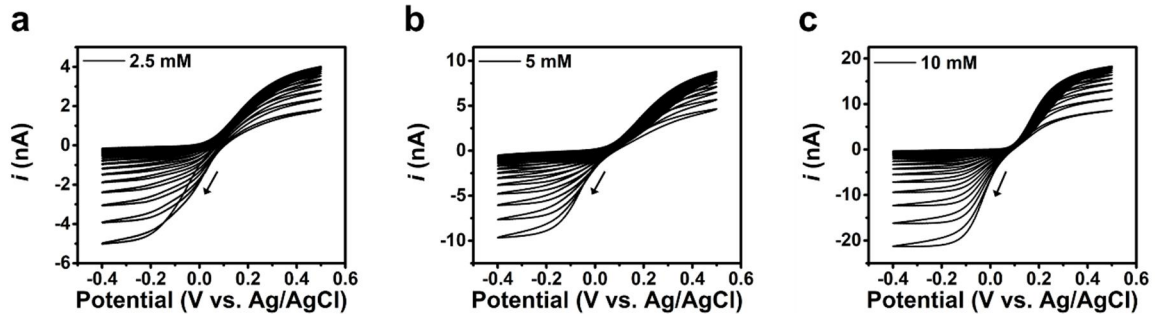

Figure S13. Successive CVs at 50 mV/s for 30 cycles over 20 minutes on a Pt UME with a radius of 5 μm in a solution, containing 1 M Im with (a) 2.5, (b) 5 and (c) 10 mM Q at pH ~ 7. The CVs were measured immediately after the injection of Im into the Q solutions, started at potential of 0.05 V and followed a negative sweep to -0.4 V, then a potential sweep to 0.5 V, and back to 0.05 V. In the process of sweeping the potential, the reduction current gradually decreases, and the oxidation current gradually increases.

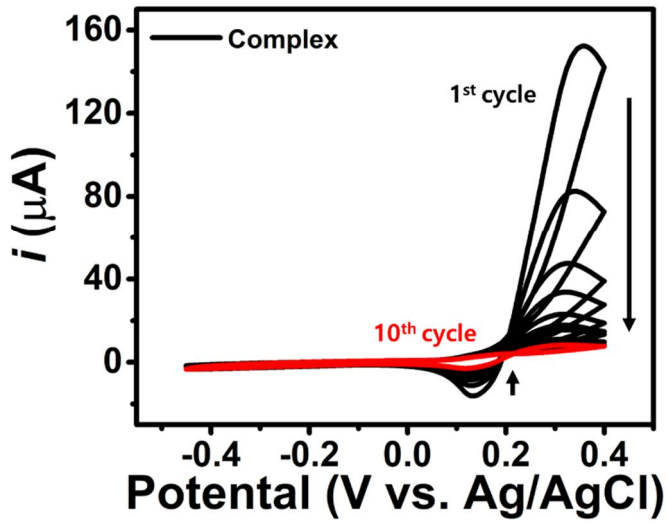

Figure S14. Successive CVs on the modified glassy carbon macrodisk electrode coated with a quinone-Im complex measured in a solution containing 1 M Im.

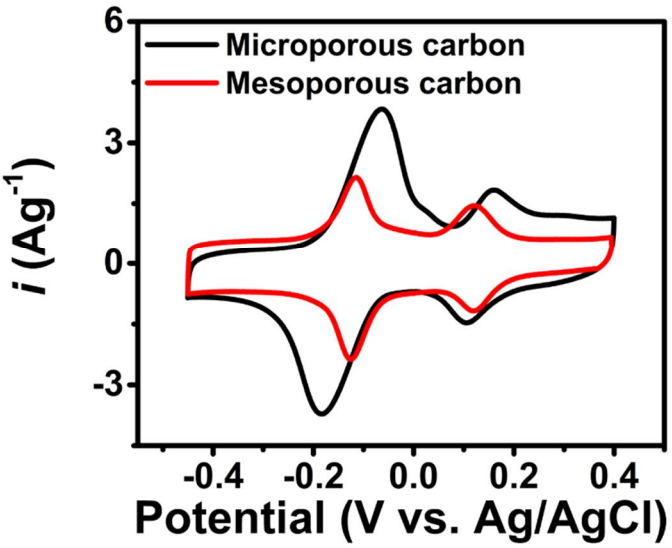

Figure S15. The 10th cycle CVs associated with H_2Q/Q redox reaction on (black) MPE and (red) ordered mesoporous carbon electrode in an aqueous solution containing 5 mM H_2Q + 1 M Im.

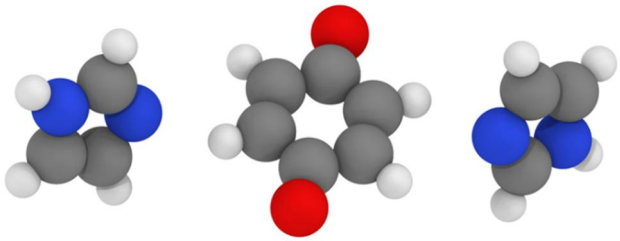

Figure S16. The structure of quinone-Im complex for ΔG_3 in DFT calculation.

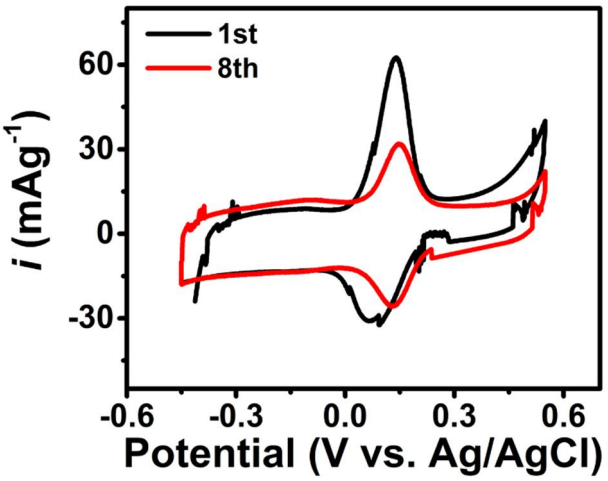

Figure S17. The successive CVs (1st and 8th cycle) at 0.1 mV/s measured from MPE (CE)|5 mM H_2Q + 1 M citrate, pH ~ 7||the same component as the other side|MPE (WE).

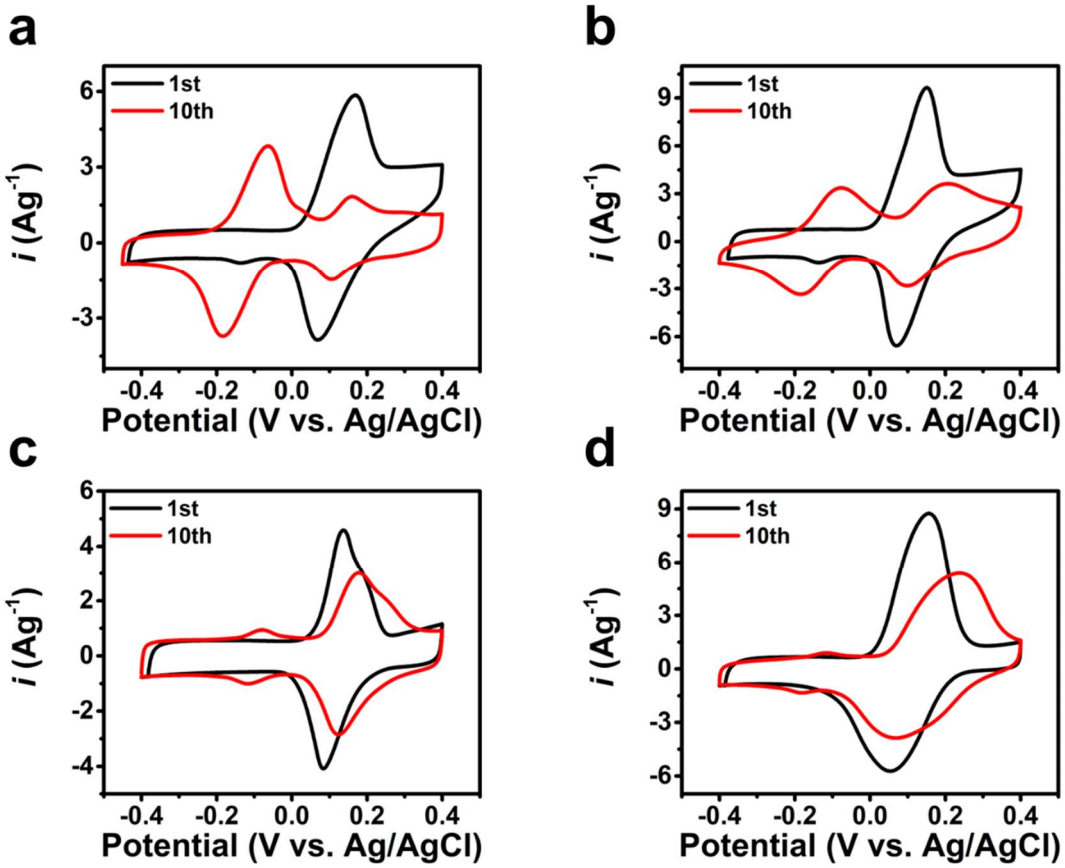

Figure S18. The 1st and 10th cycle CVs at 5 mV/s measured in the Im + citrate buffer solutions containing 5 mM H_2Q, pH ~ 7 with different f_{Im} : f_{CB} = (a) 1 : 0, (b) 0.8 : 0.2, (c) 0.5 : 0.5, and (d) 0.2 : 0.8 on MPE.

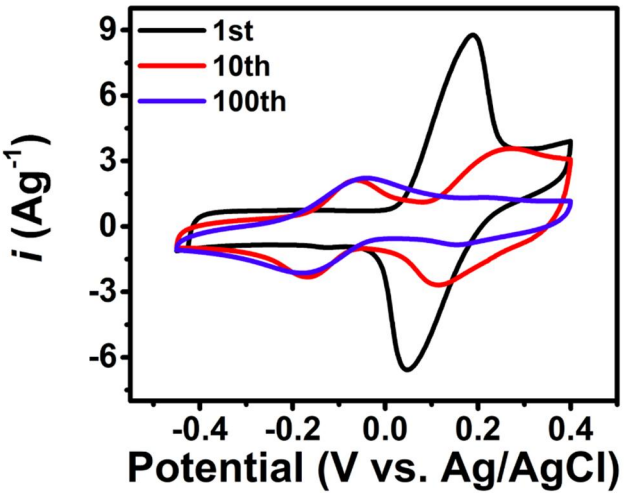

Figure S19. Successive CVs at 5mV/s measured in the 2 M Im solutions containing 10 mM H_2Q on MPE.

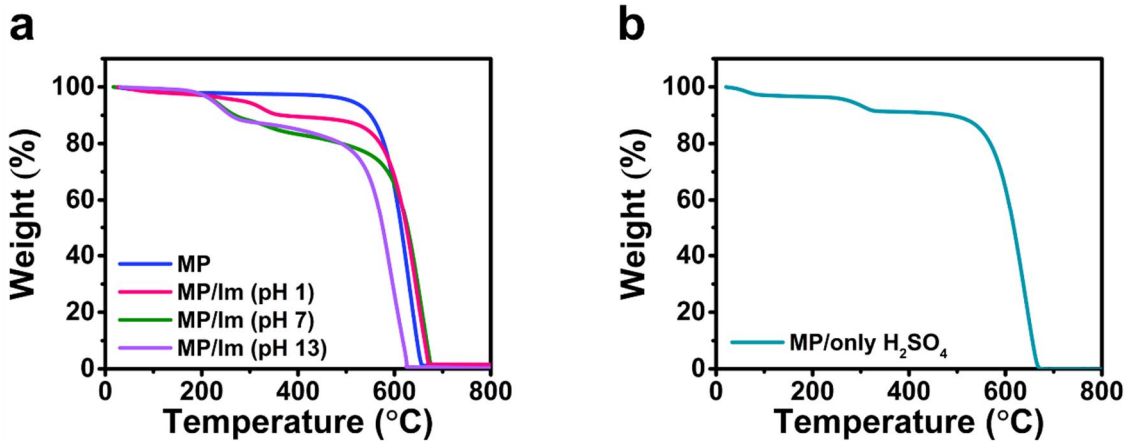

Figure S20. TGA results (a) from a pristine microporous carbon (MP) and the ones immersed in the 1 M Im solution at pH ~ 1 (acidic), 7 (neutral), and 13 (alkaline), (b) the one immersed in an acidic solution containing only H_2SO_4.

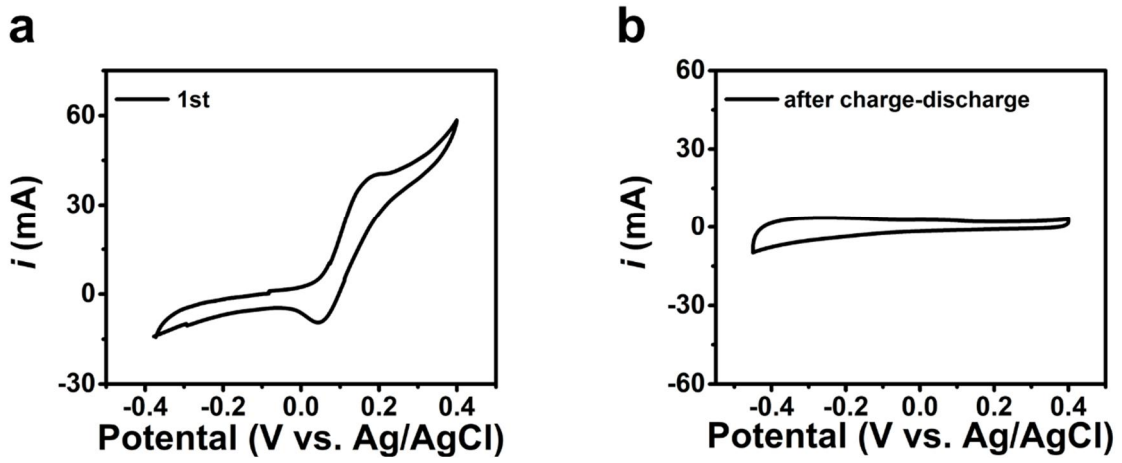

Figure S21. (a) CV measurements on a pyrolytic graphite sheet electrode in the solution, containing 5 mM H_2Q + 1 M Im, pH ~ 7, and (b) the one after the 100^{th} cycle of charge-discharge process. The scan rate of all CVs was 5 mV/s.

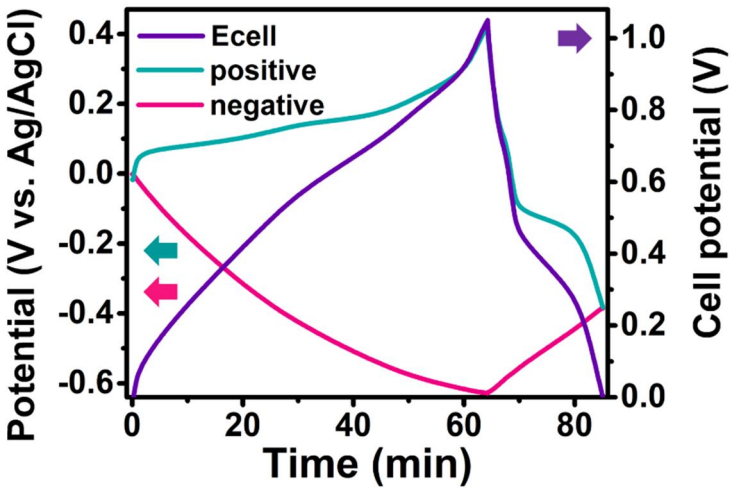

Figure S22. The 1st cycle charge and discharge curve from the cell (purple), positive (green), and negative (red) electrodes, respectively measured in (−)MPE|5 mM H_2Q + 1 M Im, pH ~ 7||using the same component as the negative electrode side|MPE(+) at 0.3A/g.

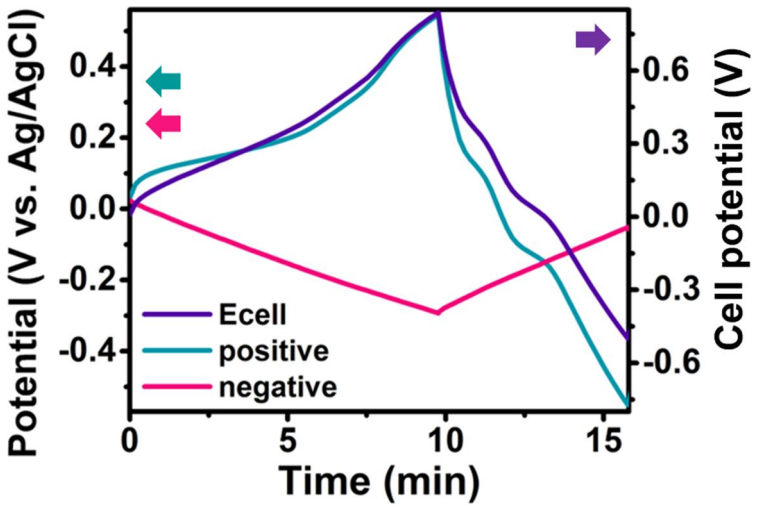

Figure S23. First cycle of charge-discharge characteristic measured in the compact-cell configured as (−) MPE|5 mM H_2Q + 1 M Im||using the same component as the other side|ordered mesoporous carbon electrode (+) at 0.5A/g.

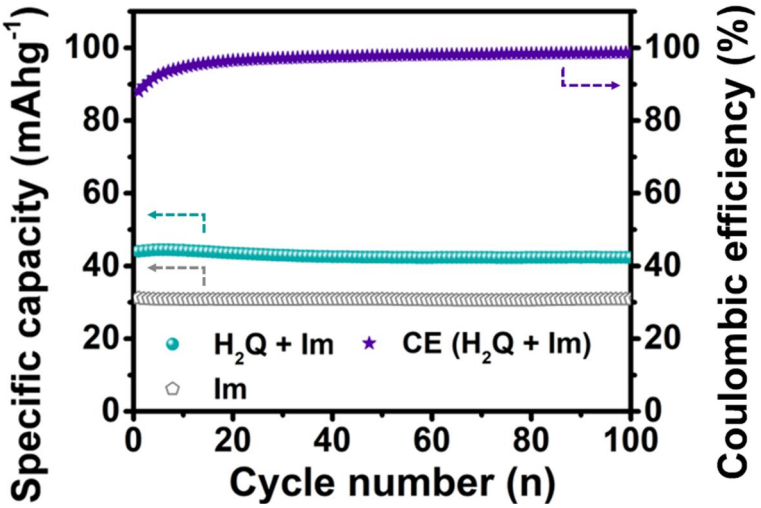

Figure S24. (left) Discharge capacity and (right) the coulombic efficiency as a function of the numbers of the charge-discharge cycles at 0.5 A/g on ordered mesoporous carbon electrode in a solution containing 5 mM H_2Q + 1 M Im.

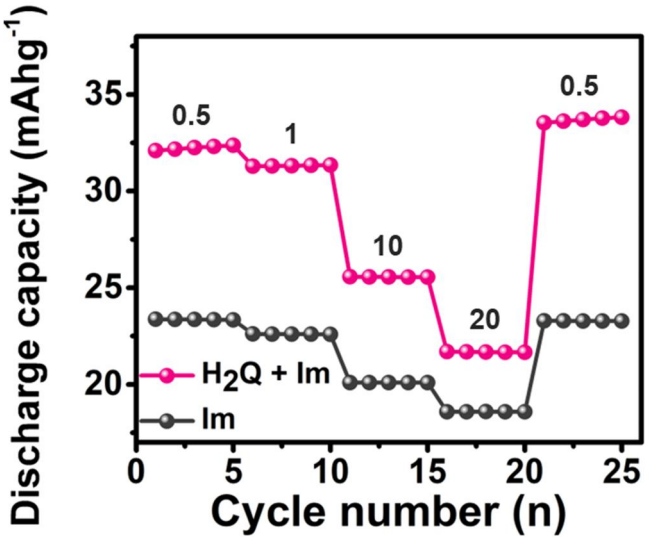

Figure S25. Discharge capacity at the ordered mesoporous carbon electrode under different current densities in 1 M Im solution with (pink)/without (black) 5 mM H_2Q after pretreatment step (5 cycles, 0.3 A/g).

Table S1. The volume of the adsorbed N_2 at monolayer (V_m), BET surface area ($a_{s,BET}$), BET constant (C), total pore volume ($V_{total\ pore}$), mesopore volume ($V_{meso\ pore}$), micropore volume ($V_{micro\ pore}$), average pore diameter ($\Phi_{average\ pore}$), median pore diameter ($\Phi_{median\ pore}$) from non-porous graphite, microporous, ordered mesoporous carbon and the microporous ones immersed in 1 M Im solutions at pH ~ 1 (acidic), 7 (neutral), and 13 (alkaline).

Sample	V_m [cm^3/g]	$a_{s,BET}$ [m^2/g]	C	$V_{total\ pore}$ [cm^3/g]	$V_{meso\ pore}$ [cm^3/g]	$V_{micro\ pore}$ [cm^3/g]	$\Phi_{average\ pore}$ [nm]	$\Phi_{median\ pore}$ [nm]
Graphite	1.7355	7.5538	176.4	0.0485	0.0481	0.0004	25.689	0.7
Microporous carbon	543.18	2364.2	412.79	1.0383	0.4257	0.6126	1.5938	0.7512
Ordered meso-porous carbon	222.82	969.83	229.78	0.9203	0.8018	0.1185	3.8	3.7955
Acidic pH	428.14	1863.5	307.34	0.8195	0.3622	0.4573	1.62	0.7634
Neutral pH	251.3	1093.8	178.01	0.4981	0.2816	0.2165	1.7995	0.8093
Alkaline pH	276.29	1202.5	237.26	0.5461	0.2839	0.2622	1.7332	0.7916

Table S2. The initial rates of the chemical reaction between Q and Im at different concentrations of Q estimated from the slopes of the C_Q*-*t* profiles (Figure 1h) from 0 to 40 s, and the corresponding pseudo-first-order rate constant.

No.	[Q] (M)	$\frac{\Delta C}{\Delta t}$ (mM/s)	Initial rate (M/s)	Rate constant k' (s^{-1})
1	0.01	$\frac{9.02-6.84}{40}$	54.5×10^{-6}	5.45×10^{-3}
2	0.005	$\frac{4.91-3.91}{40}$	25.0×10^{-6}	5.0×10^{-3}
3	0.0025	$\frac{2.34-1.83}{40}$	12.75×10^{-6}	5.1×10^{-3}

Table S3. The system components of MD simulation: the CNT diameter, the numbers associated with each molecule. The number of molecules was adjusted to keep the density the same.

System	Diameter [nm]	H_2Q	Q	Im	H_2O
H_2Q CNT	1.221	8	-	17	92
H_2Q CNT	2.032	32	-	64	356
H_2Q CNT	2.980	79	-	159	881
Q CNT	1.221	-	8	16	91
Q CNT	2.032	-	32	64	354
Q CNT	2.980	-	79	158	876

Table S4. DFT calculations to estimate the Gibbs free energy changes for stabilization of Q (ΔG_1) and Im (ΔG_2) by interaction with carbon surface, which are compared to that for formation of Q-2Im complex (ΔG_3).

No.	Reactions	Gibbs free energy change, ΔG (eV)
1	Adsorption of one Q on carbon	-0.55
2	Adsorption of one Im on carbon	-0.36
3	Formation of Q-2Im complex	-0.33

References

1. M. Quan, D. Sanchez, M. F. Wasylkiw and D. K. Smith, *J. Am. Chem. Soc.*, 2007, **129**, 12847-12856.
2. A. J. Bard, L. R. Faulkner and H. S. White, *Electrochemical methods: fundamentals and applications*, John Wiley & Sons, 2022.